Title	Improving efficiency roll-off in organic light emitting devices with a fluorescence-interlayer-phosphorescence emission architecture
Author(s)	Zheng, T; Choy, WCH; Ho, CL; Wong, WY
Citation	Applied Physics Letters, 2009, v. 95 n. 13
Issued Date	2009
URL	http://hdl.handle.net/10722/73904
Rights	Creative Commons: Attribution 3.0 Hong Kong License

Improving efficiency roll-off in organic light emitting devices with a fluorescence-interlayer-phosphorescence emission architecture

Tianhang Zheng,[1] Wallace C. H. Choy,[1,a)] Cheuk-Lam Ho,[2] and Wai-Yeung Wong[2,a)]
[1]*Department of Electrical and Electronic Engineering, The University of Hong Kong, Pokfulam Road, Hong Kong*
[2]*Department of Chemistry, Centre for Advanced Luminescence Materials, Hong Kong Baptist University, Kowloon Tong, Hong Kong*

(Received 13 July 2009; accepted 10 September 2009; published online 2 October 2009)

Organic light emitting devices (OLEDs) with a fluorescence-interlayer-phosphorescence emission layer structure (FIP EML) has been proposed to solve the efficiency roll-off issue effectively. Efficient green OLED based on FIP EML exhibiting only 26% roll-off in the luminance efficiency, which is lower than the typical roll-off of 51% for conventional phosphorescent OLEDs with single EML operated at 5–150 mA/cm^2 range, has been demonstrated. Such enhancement should be attributed to the improved carrier balance, the exciton redistribution in recombination zone, the suppression of nonradiative exciton quenching processes, and the elimination of energy transfer loss offered by the FIP EML structure. © *2009 American Institute of Physics*. [doi:10.1063/1.3241079]

Highly efficient organic light emitting device (OLED) has been studied extensively because it has great potential to save energy for lighting applications by improving energy efficiency for several times higher than that of conventional incandescent and fluorescent lamps.[1–3] With the development of phosphorescent emitters, theoretically, OLED with 100% internal quantum efficiency can be realized, and now various device architectures have been proposed to demonstrate this concept with peak external quantum efficiency around 20% in experimental levels.[4–7] However, device efficiency drops rapidly from the peak value with increasing current, and thus device has a much lower efficiency at high current, which is called efficiency roll-off effect.[8–10] Such inherent effect is quite severe in phosphorescent OLEDs and detrimentally degrades the device working performance for practical applications particularly at high luminance.

Fundamental studies have indicated that the origin of efficiency roll-off should mainly be attributed to the deterioration of charge carrier balance and the increase of nonradiative quenching processes including triplet-triplet annihilation (TTA), triplet-polaron annihilation (TPA), and electric field induced dissociation of excitons at high current density.[11–13] To solve the efficiency roll-off issue, several measures can be taken: (i) the used phosphorescent emitter should have a short decay lifetime and a small TTA rate, which are more dependent on materials properties, (ii) device architectures should be optimized to get carrier balance and minimize charge accumulation in emission layer (EML),[2,6] and (iii) the generated excitons should be confined and managed effectively by tailoring EML. In view of the above considerations, it is very critical to engineer OLED structure for reducing efficiency roll-off effect. Although some methods have been proposed presently, for instance, the adoption of mixed host,[13] doubled EML,[8,9] using new electron transport layer with high mobility,[14] and the introduction of exciton blocking layer,[10] etc., further improvement and alternative strategies are desirable.

In this letter, we report an OLED architecture by doping fluorescent- and phosphorescent-type emitters, respectively, into two different hosts to form a fluorescence-interlayer-phosphorescence structure (FIP) as EML. Green OLED with FIP EML exhibits a much lower luminance efficiency roll-off value of 26% compared with the value of 51% for conventional phosphorescent OLED with single EML in the 5–150 mA/cm^2 range. The mechanism of such improvement will be discussed.

All devices were fabricated onto indium tin oxide (ITO) coated glass substrates by thermal evaporation and the processing steps can be found elsewhere.[15] OLEDs with FIP EML have a structure of ITO(120 nm)/NPB(45 nm)/NPB: C545T(10 nm,x wt %)/CBP(10 nm)/CBP:Ir(H-Cz-py)$_3$(20 nm,7 wt %)/TPBi(40 nm)/LiF(1 nm)/Al(100 nm). The devices are named as FIP1 (x=0.5 wt % C545T), FIP2 (1 wt %), FIP3 (1.5 wt %) and FIP4 (2 wt %). Here, NPB, C545T, CBP, Ir(H-Cz-py)$_3$, and TPBi are N,N′-diphenyl-N,N′-bis(1-naphthyl)-(1,1′-biphenyl)-4,4′-diamine, 10–2-(benzothiazolyl)-2,3,6,7-tetrahydro-1,1,7,7-tetramethyl-1H,5H,11H-(1) benzopyropyrano(6,7,-8-ij)quinolizin-11-one, 4,4′-bis(9-carbazolyl)-1,1′-biphenyl, *fac*-tris[2-(9-phenylcarbazolyl)-2-pyridyl)iridium, 1,3,5-tris(N-phenylbenzimidazol-2-yl)benzene, respectively. The synthesis of Ir(H-Cz-py)$_3$ has been described in Ref. 16. Two control devices (Control 1 and 2) with single EML of NPB doped with 1.5 wt % C545T and CBP doped with 7 wt % Ir(H-Cz-py)$_3$, respectively, were also fabricated with a structure of ITO(120 nm)/NPB(45 nm)/EML(30 nm)/TPBi(40 nm)/LiF(1 nm)/Al(100 nm). The characteristics of current-voltage-luminance (J-V-L) and electroluminance (EL) spectra were measured by a Keithley 2400 source, a calibrated Si photodiode, and an Oriel spectrometer, and the absorption and the photoluminescence (PL) spectra were recorded by Hewlett-Packard 8452A and Spex Fluorolog-2 F111 spectrophotometers, respectively.

From Fig. 1, the photophysical properties of NPB:C545T and CBP:Ir(H-Cz-py)$_3$ favor the energy transfer in the host-guest systems.[1] It can be seen that a large overlap exists between the emission peak of NPB at 446 nm

a)Authors to whom correspondence should be addressed. Electronic addresses: chchoy@eee.hku.hk and rwywong@hkbu.edu.hk.

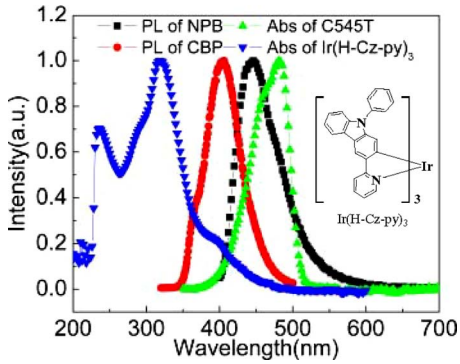

FIG. 1. (Color online) The absorption and photoluminescence spectra of two guests and two hosts, respectively. Inset: the chemical structure of $Ir(H\text{-}Cz\text{-}py)_3$.

and the absorption band of C545T at 482 nm. Meanwhile, for CBP:$Ir(H\text{-}Cz\text{-}py)_3$ system, the metal-to-ligand charge transfer bands (either singlet (^{1}MLCT) at 390 nm or triplet (^{3}MLCT) at 426 nm) can be covered in the fluorescence band between 350–500 nm of CBP. Therefore, such host-guest combinations can facilitate energy transfer through Forster- ($S_{1,NPB}$-$S_{1,C545T}$, $S_{1,CBP}$-$S_{1,Ir}$, and $S_{1,CBP}$-$T_{1,Ir}$) and Dexter-type ($T_{1,CBP}$-$T_{1,Ir}$) interactions.

Figure 2 shows the *J-V-L* characteristics of all devices. When the entire EML is doped with C545T in Control 1, the luminance efficiency (η_L) is quite low due to the initial limitation of singlet exciton quantity, but it exhibits a very low efficiency roll-off analogous to typical fluorescent-type OLEDs over the whole range of applied current.[17] For instance, η_L decreases only by about 15% between 5 and 150 mA/cm^2. However, for phosphorescent OLED of Control 2, although it has a high peak η_L of 18.5 cd/A at 1.22 mA/cm^2, its η_L drops rapidly with increasing *J*, and

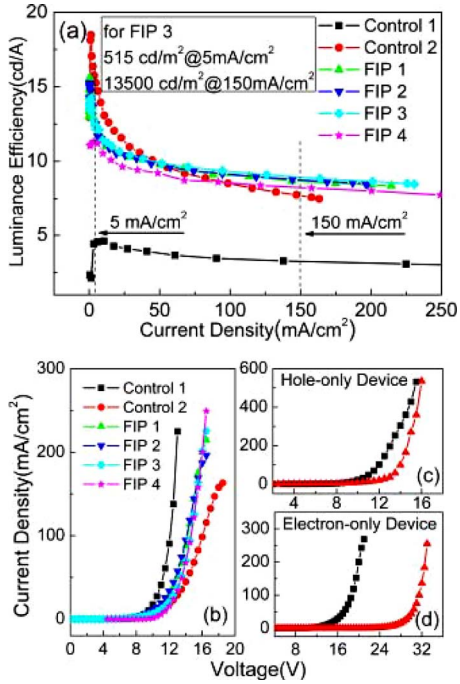

FIG. 2. (Color online) Luminance efficiency-current density (a) and current density-voltage (b) characteristics of FIP and two control OLEDs; *J-V* curves of hole-only device (c) with structures of ITO/NPB/NPB/Au/Al (square) and ITO/NPB/NPB:C545T/Au/Al (triangle), and electron-only devices (d) with structures of ITO/NPB/NPB/TPBi/LiF/Al (square) and ITO/NPB/NPB:C545T/TPBi/LiF/Al (triangle).

51% of roll-off in η_L can be observed over 5–150 mA/cm^2, which generally is attributed to the enhanced TTA process induced by a large amount of excitons at high *J*.[18]

By introducing FIP EML structure in FIP 1–4, the peak η_L becomes lower at $J<50$ mA/cm^2 and then higher at $J>50$ mA/cm^2 compared with the performance of Control 2, Thus, the efficiency roll-off of FIP OLED improves significantly with only 26% reduction within 5–150 mA/cm^2 range which is comparable to that of Control 1 (fluorescent OLED). Interestingly, the device efficiency is not affected severely and around three times higher than that of **Control 1**. We also verify this concept in red phosphorescent OLEDs with similar FIP structure. The results show that an improvement of more than 20% in the efficiency roll-off as compared to that of the phosphorescent OLEDs with single EML. When we increase the doping concentration of C545T from 0.5 to 2 wt %, FIP 1–4 have similar efficiency roll-off levels. But their η_L show two differences. First, the lower the doping concentration, the higher the peak η_L; Second, at high *J* ($J>5$ mA/cm^2), η_L increases with doping level from 0.5 to 1.5 wt %, i.e., maximized at FIP 3, and then η_L reduces quickly in FIP 4 with 2% C545T. These results demonstrate that the doping of C545T and formation of FIP EML structure definitely influence device performance which will be discussed as follows.

According to the *J-V* curves in Fig. 2(b), the carrier transport ability of FIP 1–4 is better than that of Control 2 but lower than that of Control 1. Furthermore, an increasing C545T doping level leads to the reduction of *J* at a fixed *V*. In order to understand the mechanism, another group of hole- and electron-only devices are fabricated to study the function of C545T. They have structures of ITO/NPB(45 nm)/NPB(30 nm)/Au(10 nm)/Al(100 nm) and ITO/NPB(45 nm)/NPB:C545T(30 nm, 1.5 wt %)/Au(10 nm)/Al(100 nm) for hole-only devices, and ITO/Al(20 nm)/NPB(45 nm)/NPB(30 nm)/TPBi(40 nm)/LiF(1 nm)/Al(100 nm) and ITO/Al(20 nm)/NPB(45 nm)/NPB:C545T(30 nm, 1.5 wt %)/TPBi(40 nm)/LiF(1 nm)/Al(100 nm) for electron-only devices. From Figs. 2(c) and 2(d), we can see that both the hole and electron currents are reduced upon doping C545T, especially for the electron current. Therefore, C545T molecules serve as hole and electron traps simultaneously in FIP 1–4.

In further analyzing the results, the introduction of C545T improves the balance of the electrons and holes in CPB layer. Our results show that the blocking of hole carriers by the introduction of C545 contributes to this improvement and it is considered that holes should be the majority.[19] Moreover, we know that TTA and TPA processes play a dominant role at large exciton number, i.e., high *J*, to quench the radiative emission of excitons. However, these two effects can be improved in FIP OLED. For TTA effect, FIP EML can broaden the recombination zone inside the OLEDs to reduce the density of generated triplet excitons that leads to a reduced TTA behavior.

Concerning the exciton distribution, it is considered that a large amount of excitons should be generated in CPB (as the energy transfer between CBP and $Ir(H\text{-}Cz\text{-}py)_3$ is efficient and the EL emission from $Ir(H\text{-}Cz\text{-}py)_3$ is strong) and localize and decay near the interface of EML/electron transport layer, as indicated by Arrow A in Fig. 3. As reported for some typical OLEDs,[10,20,21] the width of recombination zone

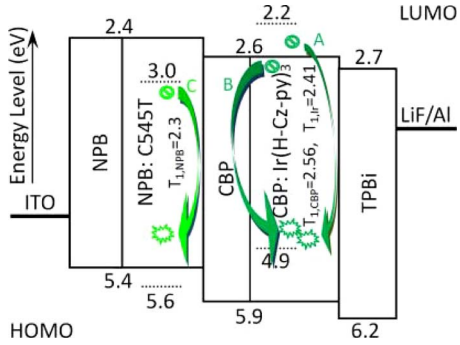

FIG. 3. (Color online) Energy level scheme of the FIP OLED, and three arrows represent the possible paths of exciton movement in recombination zone.

is $\leq$10 nm. However, some excitons could diffuse into the neat CBP interlayer due to the small energy gap (0.15 eV) between the triplet energies of CBP (2.56 eV) and $Ir(H\text{-}Cz\text{-}py)_3$ (2.41 eV), as shown in Fig. 3. It is possible that the excitons would mitigate into CBP:$Ir(H\text{-}Cz\text{-}py)_3$ zone and contribute to the emission finally because the diffusion length of triplets can be as large as about 10 nm (Ref. 22) as illustrated by the Arrow B in Fig. 3. Thus, the CBP interlayer has dual functions. One is to help extend the distribution zone of excitons to reduce TTA behavior. Another is to act as a barrier layer to block the mitigated excitons and to allow the excitons back to the CBP:$Ir(H\text{-}Cz\text{-}py)_3$ region for light emission from $Ir(H\text{-}Cz\text{-}py)_3$. Without the CPB interlayer, excitons can easily diffuse into NPB:C545T region which may result in non-radiative recombination of excitons and reduction of η_L. For TPA behavior, because the reduction of hole transport mobility caused from C545T lowers the formation of h^+ polarons, the quantity of triplet-polaron pairs is small which leads to a reduced TPA effect.

Furthermore, due to the carrier suppression role of C545T (i.e., trap carriers in NPB:C545T region), the number of excitons created in FIP 1–4 at low J becomes slightly smaller compared with that of Control 2, which results in a lower peak η_L, and such effect is more noticeable with increasing C545T doping concentration. However, for η_L at high J, the effect of the carrier suppression role of C545T becomes less important. In fact, a higher η_L for FIP 1–4 was obtained as compared to Control 2.

Finally, C545T shows light emission which can provide evidence that electrons and holes are trapped in C545T. As shown in Fig. 4, the emission of C545T in FIP 1–3 is not obvious because the spectra is pretty similar to that of Control 2, i.e., the spectra of $Ir(H\text{-}Cz\text{-}py)_3$. When the doping

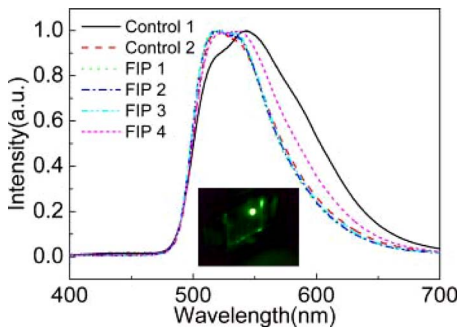

FIG. 4. (Color online) Electroluminescence spectra of the FIP OLEDs and two control devices. Inset: image of FIP3 device driven at 8 V.

concentration of C545T increases to 2 wt % in FIP 4, the spectrum stretches to the long wavelength side, indicative of the emission from C545T. The emission should come from direct recombination of holes and electrons, as indicated by Arrow C in Fig. 3, other than energy transfer from the existing triplet excitons due to the barrier of CBP layer.

In summary, we have developed an effective OLED architecture with a FIP structure as EML by doping fluorescent- and phosphorescent-type emitters respectively into two different hosts, which can greatly help reduce efficiency roll-off behavior. Green OLED based on this architecture exhibiting a much lower luminance efficiency roll-off value of 26% compared with 51% for conventional phosphorescent OLED with single EML in the 5–150 mA/cm^2 range has been demonstrated. The reasons of the enhancement have been described in detail. The scheme can be used as an effective strategy to develop efficient OLED with reduced efficiency roll-off behavior.

This work is supported under Grant No. HKU 712108 from the Research Grants Council of the HK Special Administrative Region, China. W.-Y.W. thanks the Hong Kong Research Grants Council (Grant No. HKBU 202106) and the Hong Kong Baptist University (Grant No. FRG2/08-09/111) for financial support. We would like to thank Xiaoming He for the measurements of photophysical properties of organic semiconductors.

[1]G. Schwartz, S. Reineke, T. C. Rosenow, K. Walzer, and K. Leo, Adv. Funct. Mater. **19**, 1319 (2009).
[2]G. Schwartz, T. H. Ke, C. C. Wu, K. Walzer, and K. Leo, Appl. Phys. Lett. **93**, 073304 (2008).
[3]Y. Sun, N. C. Giebink, H. Kanno, B. Ma, M. E. Thompson, and S. R. Forrest, Nature (London) **440**, 908 (2006).
[4]C. Adachi, M. A. Baldo, M. E. Thompson, and S. R. Forrest, J. Appl. Phys. **90**, 5048 (2001).
[5]Y. Kawamura, K. Goushi, J. Brooks, and J. J. Brown, Appl. Phys. Lett. **86**, 071104 (2005).
[6]F. So, B. Krummacher, M. K. Mathai, D. Poplavskyy, S. A. Choulis, and V. E. Choong, J. Appl. Phys. **102**, 091101 (2007).
[7]E. L. Williams, K. Haavisto, J. Li, and G. E. Jabbour, Adv. Mater. **19**, 197 (2007).
[8]Q. Wang, J. Ding, D. Ma, Y. Cheng, L. Wang, X. Jing, and F. Wang, Adv. Funct. Mater. **19**, 84 (2009).
[9]W. S. Jeon, T. J. Park, S. Y. Kim, R. Pode, J. Jang, and J. H. Kwon, Appl. Phys. Lett. **93**, 063303 (2008).
[10]J. W. Kang, S. H. Lee, H. D. Park, W. I. Jeong, K. M. Yoo, Y. S. Park, and J. J. Kim, Appl. Phys. Lett. **90**, 223508 (2007).
[11]S. Reineke, G. Schwartz, K. Walzer, and K. Leo, Appl. Phys. Lett. **91**, 123508 (2007).
[12]M. A. Baldo, C. Adachi, and S. R. Forrest, Phys. Rev. B **62**, 10967 (2000).
[13]N. C. Giebink and S. R. Forrest, Phys. Rev. B **77**, 235215 (2008).
[14]S. H. Kim, J. Jang, K. S. Yook, and J. Y. Lee, Appl. Phys. Lett. **92**, 023513 (2008).
[15]F. X. Zang, T. C. Sum, A. C. H. Huan, T. L. Li, W. L. Li, and F. Zhu, Appl. Phys. Lett. **93**, 023309 (2008).
[16]T. Zheng, W. C. H. Choy, and Y. Sun, Appl. Phys. Lett. **94**, 123303 (2009).
[17]W. Y. Wong, C. L. Ho, Z. Q. Gao, B. X. Mi, C. H. Chen, K. W. Cheah, and Z. Y. Lin, Angew. Chem., Int. Ed. **45**, 7800 (2006).
[18]T. Y. Chu, J. F. Chen, S. Y. Chen, C. J. Chen, and C. H. Chen, Appl. Phys. Lett. **89**, 053503 (2006).
[19]C. J. Liang and W. C. H. Choy, Appl. Phys. Lett. **89**, 251108 (2006).
[20]W. Y. Hung, T. H. Ke, Y. T. Lin, C. C. Wu, T. H. Hung, T. C. Chao, K. T. Wong, and C. I. Wu, Appl. Phys. Lett. **88**, 064102 (2006).
[21]S. Reineke, K. Walzer, and K. Leo, Phys. Rev. B **75**, 125328 (2007).
[22]E. B. Namdas, A. Ruseckas, I. D. W. Samuel, S. C. Lo, and P. L. Burn, Appl. Phys. Lett. **86**, 091104 (2005).